High-pressure Raman spectroscopic study of zirconium tungstate

2001 J. Phys.: Condens. Matter 13 11573

(http://iopscience.iop.org/0953-8984/13/50/316)

INSTITUTE OF PHYSICS PUBLISHING JOURNAL OF PHYSICS: CONDENSED MATTER

J. Phys.: Condens. Matter **13** (2001) 11573–11588 PII: S0953-8984(01)26436-4

High-pressure Raman spectroscopic study of zirconium tungstate

T R Ravindran[1], **Akhilesh K Arora**[1,3] **and T A Mary**[2]

[1] Materials Science Division, Indira Gandhi Centre for Atomic Research, Kalpakkam 603 102, TN, India
[2] Materials Technology Division, Indira Gandhi Centre for Atomic Research, Kalpakkam 603 102, TN, India

E-mail: aka@igcar.ernet.in

Received 3 July 2001, in final form 17 September 2001
Published 30 November 2001
Online at stacks.iop.org/JPhysCM/13/11573

Abstract

Raman spectroscopic measurements on negative-thermal-expansion (NTE) material zirconium tungstate $Zr(WO_4)_2$ at 20 K over the complete range of phonon frequencies yield 39 out of the predicted 54 optical phonons. The modes are assigned as lattice modes, and translational, librational and internal modes of the WO_4 ion. High-pressure measurements in a diamond anvil cell (DAC) have revealed that in addition to the low-frequency rigid-unit modes (RUMs) several other phonons, including the bending modes of the WO_4 ion, also exhibit negative Grüneisen parameter in the cubic phase. In the high-pressure orthorhombic phase above 0.3 GPa splitting of phonon modes is found to be consistent with the lowering of symmetry. Pressure-induced amorphization in this system at 2.2 ± 0.3 GPa is argued to arise because a pressure-induced decomposition of the compound into a mixture of ZrO_2 and WO_3 is kinetically constrained. The temperature dependence of specific heat and thermal expansion coefficient are calculated and compared with reported results. In contrast to earlier models and calculations, which considered only the phonons below 8 meV (64 cm^{-1}) to explain the NTE, it is shown that modes much higher than 8 meV also contribute significantly to NTE in this material.

1. Introduction

Several compounds have been found to exhibit negative thermal expansion (NTE). Compounds such as rubidium iodide [1], ice [2], cuprous oxide [3] and tetrahedral semiconductors [4] show NTE at low temperatures while some others such as quartz [5], aluminium phosphate [6] and lead titanate [7] exhibit NTE only at high temperatures. The NTE found in these systems

[3] Corresponding author.

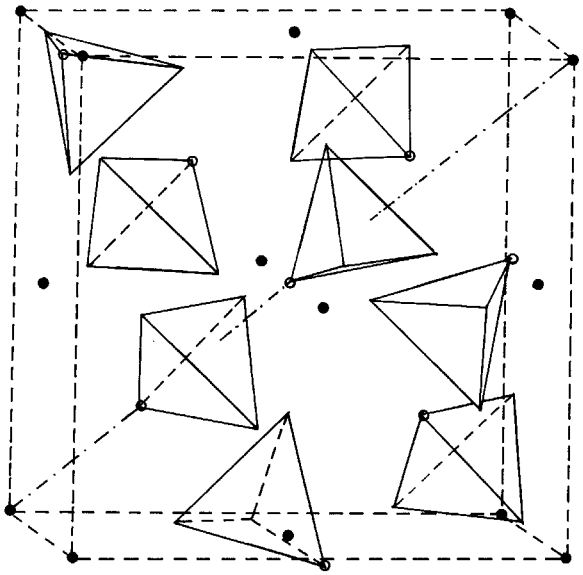

Figure 1. Cubic unit cell of zirconium tungstate. Zirconium atoms occupy the corners and the face centres. The WO_4 ions are represented by tetrahedra. The terminal oxygen lying on the C_3 axis and bonded only to W is shown as an open circle at the vertex of the tetrahedra.

is often anisotropic and strongly temperature dependent. Most of these systems consist of corner-linked polyhedral units. NTE in these systems is believed to arise due to rotation of polyhedra in a manner that pulls the entire structure inward. On the other hand, in ionic compounds such as RbI a transverse displacement of the heavy atom has been identified to be responsible for bringing the lighter atoms closer, resulting in the NTE. Although NTE in zirconium tungstate, $Zr(WO_4)_2$, had been known for some time [8], the recent synthesis of single-phase material and the report of 'large and isotropic' NTE over a wide temperature range [9] has generated considerable current interest in this system. As a consequence, a series of tungstates [10, 11] ($Y_2(WO_4)_3$, $Hf(WO_4)_2$) and molybdates [12, 13] ($Zr(MoO_4)_2$, $Sc_2(MoO_4)_3$) have been examined for possible NTE. Among these, $Zr(WO_4)_2$ has the largest magnitude of NTE.

Zirconium tungstate crystallizes in the cubic $P2_13$ (T^4) structure (α-phase) with four formula units per unit cell. Zirconium atoms occupy face-centred cubic sites while eight tungstate (WO_4) tetrahedra are located at C_3 sites. As each zirconium atom has six oxygen neighbours, the structure is also viewed as a network of corner sharing ZrO_6 octahedra and WO_4 tetrahedra [11]. Figure 1 shows the cubic unit cell. It may be mentioned that only three of the four oxygens of the WO_4 tetrahedra are shared with the neighbouring Zr ions, while the fourth oxygen, also known as the 'terminal oxygen', is bonded only to W and has significantly shorter W–O bond-length (1.73 Å) as compared with the other three W–O bonds (1.78 Å). The shorter W–O bond lies along the threefold axis and the terminal oxygen is found to have large thermal amplitude of vibration. The compound undergoes an order–disorder transition at 428 K to another cubic structure $Pa\bar{3}$, that has much higher oxygen mobility. A recent adiabatic scanning calorimetric study has shown that this transition is associated with a heat capacity anomaly [14] with a transition entropy of 2.1 J K^{-1} mol^{-1}, which is much smaller than that expected for an order–disorder transition. Raman spectroscopic studies [11] have revealed the internal modes of WO_4 ions and also the lattice modes. An irreversible structural transition to orthorhombic (γ) phase between 0.2 and 0.4 GPa has been found from high-pressure

neutron diffraction studies [15]. In the orthorhombic phase ($P2_12_12_1$) cell tripling takes place along the b-axis and one-third of the WO_4 units are found inverted [16]. Lattice dynamical calculations [17] suggest the possibility of an intermediate phase between α- and γ-phases. Subsequent energy dispersive x-ray diffraction studies revealed a gradual amorphization of the γ-phase between 1.5 and 3.5 GPa [18]. Raman spectroscopic measurements on pressure-quenched samples were used to identify some of the high-frequency (>200 cm^{-1}) modes characteristic of the orthorhombic phase. However, a systematic investigation of the pressure dependence of phonon frequencies was not carried out.

Recently we have reported the first measurement of mode Grüneisen parameter of phonons over the complete range of phonon energies and identified the phonons that contribute significantly to the NTE [19]. In this paper we report the detailed high-pressure Raman spectroscopic investigation of the cubic to orthorhombic phase transition and amorphization in $Zr(WO_4)_2$. Using the Grüneisen parameter and the reported phonon density of states, thermal properties such as specific heat C_V and thermal expansion coefficient α and their temperature dependences are obtained and compared with reported results. Possible reasons for the occurrence of pressure-induced amorphization in this system are also examined from the point of view of a kinetically hindered decomposition.

2. Experiment

Samples of $Zr(WO_4)_2$ were synthesized from appropriate quantities of $ZrOCl_2 \cdot 8H_2O$ and H_2WO_4 using a procedure [9] described earlier. Powder x-ray diffraction analysis showed that the compound was single phase. High-pressure Raman measurements were carried out on unoriented single-crystal bits in a gasketed diamond anvil cell (DAC) of 600 μm culet diameter in the back-scattering geometry using a set-up described [20] elsewhere. A hardened stainless steel gasket was pre-indented before drilling a 250 μm hole at the centre. A 4:1 mixture of methanol and ethanol was used as the pressure transmitting medium. Pressure inside the DAC was measured using a standard ruby fluorescence technique. About 100 mW power of the 488 nm line of an argon ion laser was used for exciting the Raman spectra. Low-temperature Raman spectra were measured using a closed-cycle refrigerator in the back-scattering geometry. Scattered light was analysed using a Spex double monochromator and detected using a cooled photomultiplier tube operated in the photon counting mode.

3. Results and discussion

3.1. Raman spectrum and mode assignment

As mentioned earlier, the cubic phase of $Zr(WO_4)_2$ has four formula units per unit cell. This results in 44 atoms in the unit cell and consequently a total of 132 degrees of freedom, which manifest themselves as acoustic and optic phonons. In order to calculate the number of modes of different symmetries (irreducible representations) one can treat either ZrO_6 or WO_4 as the polyatomic unit. It may be mentioned that the internal modes associated with tungstate (WO_4) tetrahedral ions [21] have been observed in the Raman spectrum of zirconium tungstate while those of ZrO_6 were not found. This suggests that WO_4 is a much more strongly bound molecular ion-like unit in this material as compared with ZrO_6. In view of this the chemical formula for this compound when written as $Zr(WO_4)_2$ appears more communicative than the commonly used one ZrW_2O_8 and it is appropriate to treat WO_4 as the polyatomic unit for the factor group analysis [22]. The phonons in this system can be classified as acoustic, lattice modes arising from Zr atom motion, translational and librational (hindered

rotation) modes of WO_4 ions and internal modes of distorted WO_4 tetrahedra. The irreducible representations associated with various classes of modes are as follows: $\Gamma_{\text{acoustic}}(3) = F$; $\Gamma_{\text{lattice}}(9) = A + E + 2F$; $\Gamma_{\text{trans}}(24) = 2A + 2E + 6F$; $\Gamma_{\text{libr}}(24) = 2A + 2E + 6F$; $\Gamma_{\text{int}}(72) = 6A + 6E + 18F$ and $\Gamma_{\text{total}}(132) = 11A + 11E + 33F$.

All the 54 optical phonons are Raman active. A tetrahedral molecular ion has four [23] internal modes; symmetric stretching (ν_1), antisymmetric stretching (ν_3), antisymmetric bending (ν_4) and symmetric bending mode (ν_2). Their frequencies for a free tungstate ion [24] are close to 930, 830, 405 and 320 cm^{-1} respectively. The modes of the free ion exhibit splitting due to lower site symmetry. In addition, the presence of eight tungstate ions in the unit cell leads to correlation or Davydov splitting of the internal modes. The correspondence between the modes of a free ion and those present in the crystal obtained using a correlation diagram [22] allows one to obtain the number of modes of different symmetries associated with each of the internal modes of the tungstate ions in the crystal. The 72 internal degrees of freedom distributed among 30 modes can be separated into four groups corresponding to ν_1 to ν_4 modes as $\nu_1(8A) \rightarrow 2A + 2F$; $\nu_3(8F_2) \rightarrow 2A + 2E + 6F$; $\nu_4(8F_2) \rightarrow 2A + 2E + 6F$ and $\nu_2(8E) \rightarrow 2E + 4F$. As these modes correspond to different regions of the phonon frequencies, one can easily identify them in the Raman spectrum.

Figure 2 shows the Raman spectrum of $Zr(WO_4)_2$ at 20 K. A total number of 39 modes are observed as compared with the predicted 54 modes. The appearance of fewer modes may be due to accidental degeneracy or insufficient intensity. At ambient temperature only 21 modes could be distinctly seen. In earlier measurements Evans *et al* [11] could find 18 modes at ambient temperature while Perottoni and Jornada [18] reported only 13 modes. Table 1 lists the mode frequencies observed in this study and those reported earlier. Note that there is a good agreement between the phonon frequencies found in this work and those reported earlier. Another remarkable feature of this material is the complete absence of any modes between 440 and 620 cm^{-1}. Similar gaps have been reported in the phonon density of states measured using neutron scattering [25] and also in that obtained from lattice dynamical calculations [26]. This renders the identification and separation of ν_2 and ν_4 internal modes from ν_3 and ν_1 modes rather straightforward. Thus the modes in the high-frequency region (628–1034 cm^{-1}) can be assigned to ν_1 and ν_3 modes alone of the tungstate ion. The symmetric and antisymmetric stretching vibrations of the tungstate ion (WO_4) are essentially those of oxygen around the central tungsten atom. One expects a total of 14 modes in this region; however, a total of 20 modes were found. This may be due to the LO–TO splitting of the infrared active phonons of symmetry F. Note that there are eight F modes expected in this region. In addition, some overtone and combination modes may also be present. The modes below 443 cm^{-1} correspond to ν_4 and ν_2 internal modes of the WO_4 ion, lattice modes and the translational and the librational modes of the tungstate ion. As there may be some overlap between the frequencies of these classes of modes, an unambiguous assignment of modes is not straightforward. Based on the frequencies of ν_2 and ν_4 modes of the WO_4 ion in other crystals [21, 24], one can tentatively assign modes between 250 and 320 cm^{-1} to ν_2 modes and those between 320 and 470 cm^{-1} to ν_4 modes of the WO_4 ion. One can also note that the total number of modes expected in the low-frequency region is 40; however, only 19 modes could be found in this study. This may be due to accidental degeneracy of mode frequencies or the presence of weak modes of intensities below the detection limit. An alternative interpretation for the appearance of more modes in the high-frequency region and absence of some modes in the low-frequency region could be a possible transfer of modes from the low-frequency to the high-frequency region; however, this appears unlikely as this would imply substantial increase in the frequencies of ν_2 and ν_4 internal modes.

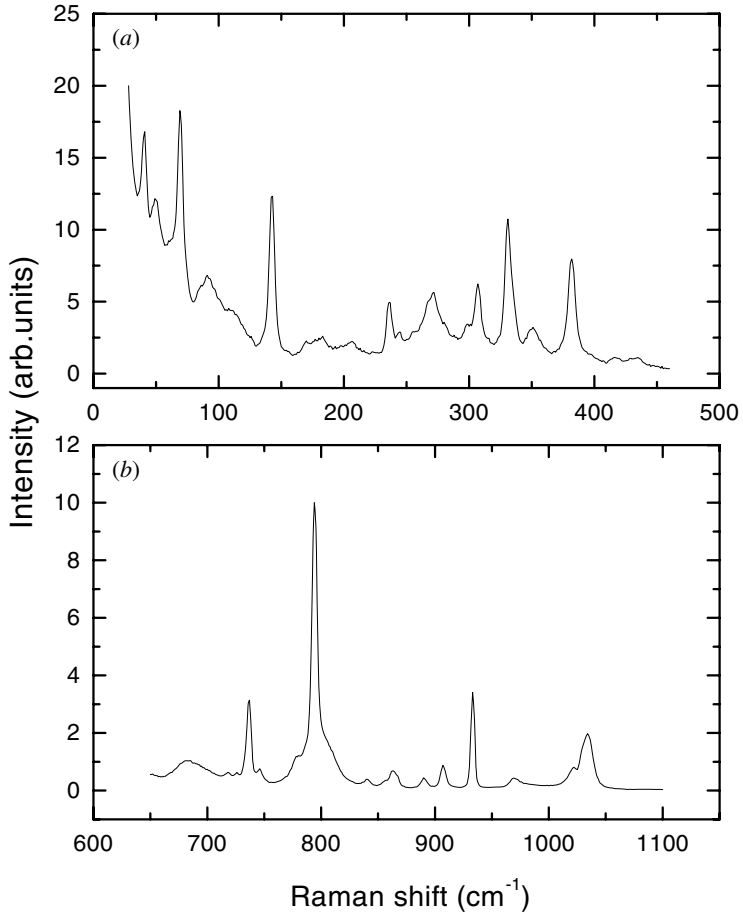

Figure 2. Raman spectrum of zirconium tungstate at 20 K. (*a*) Low-frequency region; (*b*) high-frequency region. No modes are found between 440 and 620 cm^{-1}. The high-frequency region contains only ν_3 and ν_1 internal modes of WO_4 ions.

3.2. Cubic to orthorhombic phase transition

As mentioned in the introduction, the cubic to orthorhombic transition at 0.3 ± 0.1 GPa was studied earlier using neutron diffraction [15, 16] and x-ray diffraction [27]. A coexistence region between 0.2 and 0.4 GPa was concluded from the intensities of diffraction lines and the phase transition was found to be irreversible. Taking advantage of the irreversibility of the transition, the Raman spectrum of the recovered sample after pressure release has also been measured [18]. The orthorhombic phase, also known as the γ-phase, is also found to exhibit NTE. However, NTE exists only below 225 K and the γ-phase transforms [28] to the α-phase upon heating above 390 K. The space group of γ-$Zr(WO_4)_2$ is identified as $P2_12_12_1(D_2^4)$ and the unit cell contains 12 formula units. As a consequence the number of phonon modes also becomes very large. In addition, due to lowering of crystal symmetry from cubic to orthorhombic, all doubly and triply degenerate modes split to yield nondegenerate modes. Factor group analysis yields $99A + 98B_1 + 98B_2 + 98B_3$ optical phonons, all of which are Raman active.

Table 1. Observed Raman frequencies in the cubic phase of $Zr(WO_4)_2$.

Ref. [11] (cm^{-1})	Ref. [18] (cm^{-1})	Present work (cm^{-1}) 298 K	20 K	Assignment
40	—	41	41	↑
—	—	—	50	Lattice
65	—	65	69	
—	—	74	—	+
84	—	84	91	
103	—	—	113	trans.
144	—	144	143	
—	—	—	170	+
—	—	—	181	
—	—	—	205	libr.
234	236	235	236	
—	—	244	243	↓
271	—	—	270	↑
—	—	—	298	$\nu_2(WO_4)$
308	308	310	307	↓
331	334	333	331	↑
—	—	—	350	
382	384	382	382	$\nu_4(WO_4)$
—	—	—	417	
—	—	—	433	↓
—	—	—	628	↑
—	—	—	645	
—	—	—	685	
—	—	—	718	
—	—	—	725	$\nu_3(WO_4)$
733	735	736	737	
—	—	746	747	
—	—	773	779	
789	790	790	794	
—	—	—	807	
—	—	—	841	
—	—	—	855	
859	866	861	863	
887	887	886	890	
901	902	904	907	↓
929	930	932	933	↑
966	969	967	970	$\nu_1(WO_4)$
—	—	—	987	
—	1019	1019	1021	
1028	1029	1030	1034	↓

Figure 3 shows the Raman spectra of zirconium tungstate at several pressures. Although 39 modes were observed in the spectrum at 20 K, only 21 peaks could be followed as a function of pressure at ambient temperature from the sample inside the DAC. In the γ-phase, dramatic splitting of the degenerate ν_3 mode of the WO_4 ion into a large number of components is evident from the spectra recorded at 1.27 GPa. This is consistent with the predictions of group theory. The pressure dependence of the phonon frequencies is shown in figure 4. Note that several of

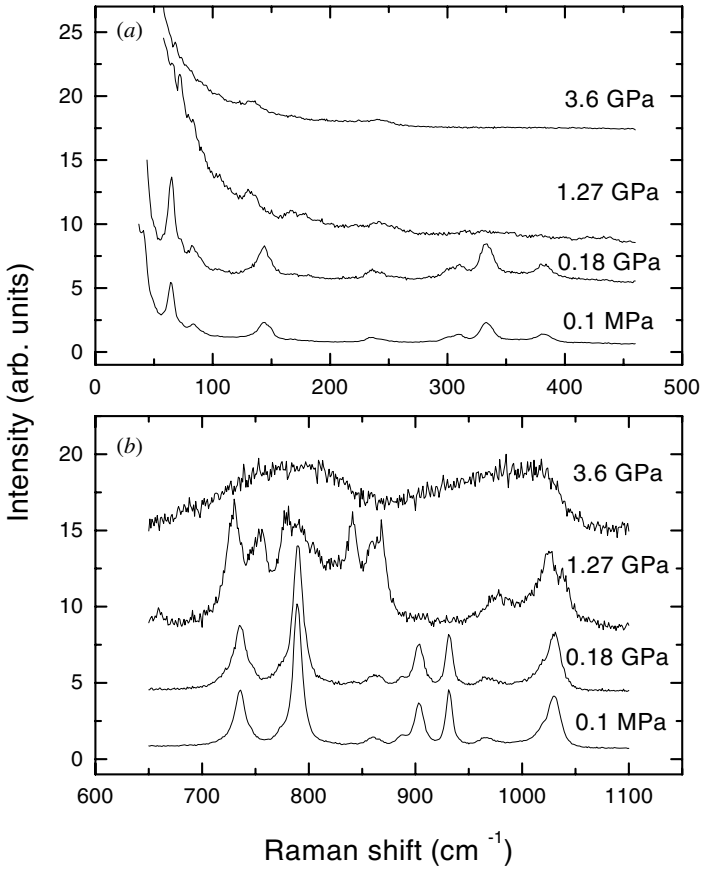

Figure 3. Raman spectrum of $Zr(WO_4)_2$ at several pressures at ambient temperature. (*a*) Low-frequency region; (*b*) high-frequency region.

the mode frequencies change discontinuously across the α–γ transition. Some of the modes characteristic of α- and γ-phases coexist between 0.2 and 0.3 GPa, confirming the coexistence of these phases reported earlier. In addition, a large number of modes in the α-phase and some in the γ-phase are found to exhibit negative slope in the ω versus P plot (figure 4). A decrease in the phonon frequency as a function of pressure often suggests 'mode softening', which is known to cause lattice instabilities [29] and consequently drive [30, 31] phase transitions. However, the mode softening found in this study for zone-centre phonons is only marginal. On the other hand, cell tripling along the b-axis across the transition suggests that softening of a phonon at $(1/3)q_B$, where q_B is the wavevector corresponding to the Brillouin-zone boundary, could be responsible for the transition at high pressure. The negative slope of the ω versus P curves also implies negative mode Grüneisen parameters γ_i, which are key factors for determining thermal properties such as thermal expansion. This is discussed in detail in a subsequent section.

3.3. Pressure-induced amorphization

In the γ-phase, when the pressure is increased further, above 1.9 GPa the lattice and external modes disappear and internal modes exhibit excessive broadening. Note the existence of broad bands in the region of ν_3 and ν_1 modes of tungstate ions in the spectra of 3.6 GPa in figure 3.

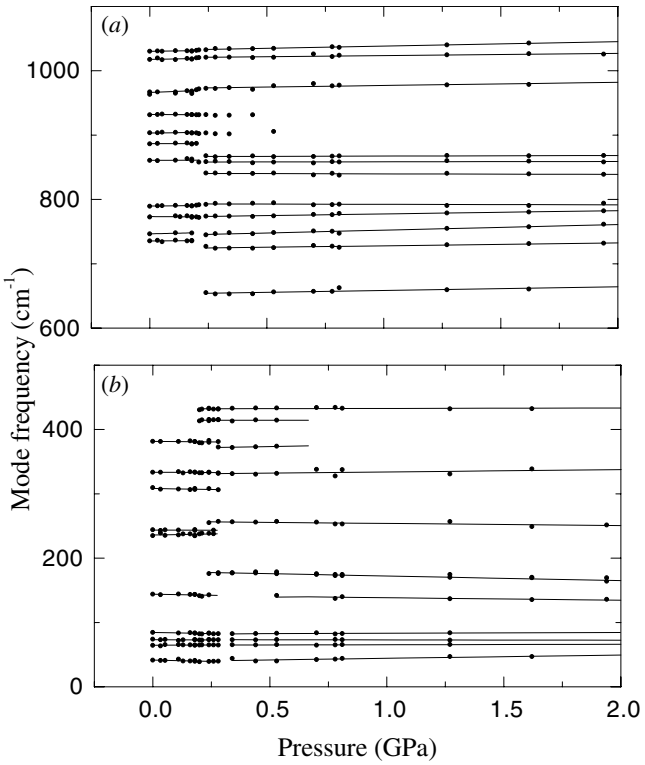

Figure 4. Pressure dependence of mode frequencies in zirconium tungstate. (*a*) High-frequency region; (*b*) low-frequency region. The discontinuous changes in the mode frequencies take place across the cubic to orthorhombic (α–γ) phase transition.

Broadening of internal modes is expected across amorphization [32, 33] because the bond-lengths and bond-angles of polyatomic units now have distribution in an amorphous phase in contrast to those being unique as in the crystalline phase. In addition, the lattice and the external modes are expected to disappear [34] due to lack of long-range order/periodicity. Thus, the observed changes in the Raman spectra could arise due to pressure-induced amorphization (PIA). From the energy dispersive x-ray diffraction studies the orthorhombic γ-phase of $Zr(WO_4)_2$ was earlier reported [18] to amorphize gradually between 1.5 and 3.5 GPa. The Raman spectrum of the recovered sample after the pressure release suggested that the amorphization was irreversible. From the present measurements we find that amorphization occurs between 1.9 and 2.4 GPa.

It may be mentioned that a few other polyhedral network systems such as quartz and ice, which show NTE over a limited range of temperatures, are also found [35, 36] to amorphize when subjected to high pressure. Recent computer simulation studies have examined the possibility of a common origin [37] for the two phenomena in tetrahedrally bonded networks. Guided by the results on zirconium tungstate, the tetrahedral network model has been argued to be valid also for tetrahedral–octahedral network structures [18]. Although it is generally accepted that PIA arises due to kinetic hindrance of equilibrium phase transitions to another crystalline structure [35], the final phases have remained speculative or unknown in most instances. Based on reports of pressure-induced decomposition (PID) in a number of complex network systems [38–40] such as Fe_2SiO_4, $CuGeO_3$ and Mg_2SiO_4 into a mixture of simple

oxides at high temperature and high pressure (HP–HT) and the observation of PIA in these systems [41–43] at ambient temperature, a new model [44] of amorphization that 'it could also arise from the kinetic hindrance of an equilibrium decomposition' has been proposed recently. The necessary condition for decomposition to occur at high pressure is that the total volume of the daughter phases must be less than that of the parent phase. If n_0 moles of the parent compound with volume V_0 per formula unit decompose to yield n_j moles of the jth daughter compound with volume V_j per formula unit, then the total volumes of the parent and daughter compounds can be written as

$$V_{\mathrm{P}} = n_0 V_0$$

and

$$V_{\mathrm{D}} = \Sigma_j n_j V_j$$

where the sum is over all the species of daughter compounds. The condition for decomposition then becomes [45] $\Delta V = V_{\mathrm{D}} - V_{\mathrm{P}} < 0$. It is worth examining whether zirconium tungstate also satisfies this criterion. For this, one may consider decomposition of the compound into a mixture of the oxides of zirconium and tungsten according to the reaction

$$\mathrm{Zr(WO_4)_2} \rightarrow \mathrm{ZrO_2} + 2\mathrm{WO_3}.$$

Using the reported unit cell volume data of zirconium tungstate and those oxides we obtain $V_{\mathrm{P}} = 191.94$ Å^3 and $V_D = 140.66$ Å^3. Thus the volume decrease upon decomposition turns out to be rather large (51.28 Å^3), which is about 27% of the original volume. This analysis thus predicts that the compound is very likely to exhibit decomposition under suitable HP–HT conditions, and the PIA found at ambient temperature arises most likely due to the kinetic hindrance of decomposition rather than a phase transition. As there exists an intermediate orthorhombic phase, which has about 5% lower volume than the cubic phase, the actual volume change upon decomposition of orthorhombic phase would be around 23%. A recent report [27] of amorphization of zirconium tungstate at high pressure and moderate temperatures ($P = 1.0$ GPa and $T \leqslant 600$ K) and decomposition at high pressure and elevated temperatures ($P = 0.6$ GPa and $T \geqslant 800$ K) indeed confirms the present model of pressure-induced amorphization and decomposition. One could in principle look for signatures of the daughter compounds in the Raman spectra. Tungsten tri-oxide exhibits characteristic Raman peaks at 710 and 816 cm^{-1} [46]. However, as there is not sufficient kinetics at ambient temperature, appearance of daughter compounds in the form of a disordered assemblage of macroscopic phases is not expected to occur in the present case. At ambient temperature the initiation of the process of decomposition at atomic or microscopic level eventually results in the amorphous phase. One can also examine whether other members of the family of tungstates [10, 11] and molybdates [12, 13, 47] such as $\mathrm{Hf(WO_4)_2}$, $\mathrm{Zr(MoO_4)_2}$, and $\mathrm{Sc_2(MoO_4)_3}$, $\mathrm{Y_2(WO_4)_3}$, which have been reported to exhibit NTE over a limited range of temperature, are likely candidates for a possible decomposition. Table 2 gives the estimated volume change for the decomposition into mixture of simple oxides. Note that all these systems have negative ΔV, suggesting that these compounds could also decompose when subjected to suitable HP–HT conditions. A calculation of ΔV for a number of compounds which exhibit PIA has suggested [44] negative ΔV as a new criterion for predicting PIA at ambient temperature. In view of this correlation, all these tungstates and molybdates are also likely to amorphize when subjected to high pressure at ambient temperature.

3.4. Grüneisen parameter and thermal expansion

As mentioned earlier, the mode Grüneisen parameters γ_i of all the phonons contribute to the thermal expansion coefficient α (see equations (1)–(3) of [19]). A negative average Grüneisen

Table 2. Calculated volume change upon decomposition of some tungstates and molybdates into mixtures of simple oxides.

Compound	Structure	V_P (Å^3)	Decomposition products	$\Delta V/V_P$ (%)
$Zr(WO_4)_2$	Cubic	191.9	$ZrO_2 + 2WO_3$	−26.7
$Hf(WO_4)_2$	Cubic	190.3	$HfO_2 + 2WO_3$	−26.4
$Zr(MoO_4)_2$	Trigonal	173.8	$ZrO_2 + 2MoO_3$	−21.4
$Y_2(WO_4)_3$	Orthorhombic	350.2	$Y_2O_3 + 3WO_3$	−33.5
$Sc_2(WO_4)_3$	Orthorhombic	304.2	$Sc_2O_3 + 3WO_3$	−28.4
$Sc_2(MoO_4)_3$	Orthorhombic	304.8	$Sc_2O_3 + 3MoO_3$	−30.5

Table 3. Mode Grüneisen parameters of various mode frequencies of cubic $Zr(WO_4)_2$. The reported value [16] of $B = 72.5$ GPa is used in the calculation. Numbers in the parentheses represent the standard errors in the least significant digits.

Mode frequency (cm^{-1})	Phonon energy (meV)	γ_i
41	5.1	−14(3)
65	8.1	2.4(17)
74	9.2	−1.5(10)
84	10.4	−7(2)
144	17.9	−3(2)
235	29.1	2(1)
244	30.3	−0.2(6)
310	38.4	−1.5(9)
333	41.3	−0.4(5)
382	47.4	−0.7(8)
736	91.3	0.2(5)
746	92.5	1(1)
773	95.8	0.1(4)
790	98.0	0.9(3)
861	107.0	0.7(6)
886	110.0	0.0(3)
904	112.0	−0.1(3)
967	120.0	1.4(4)
1019	126.3	0.7(2)
1030	128.0	0.7(2)

parameter γ_{AV} implies NTE. Although γ_i may be temperature independent, the T-dependence of γ_{AV} emerges from the temperature dependences of Einstein specific heats C_i associated with the ith mode. In addition, if some of the γ_i are positive and others negative, there may be cancellation of the contributions from different γ_i to the average Grüneisen parameter and consequently to α. In $Zr(WO_4)_2$, the pressure range of stability of the cubic phase is rather small. In order to make reliable estimates of mode Grüneisen parameter γ_i, measurements were made at close intervals of pressure. In addition, data from several pressure runs were analysed. The peak positions of Raman lines were obtained using a nonlinear least-squares fitting program. The slope of ω versus P curves and their standard errors were obtained from a linear least-squares fit to the data. The straight lines in figure 4 represent the linear fits to the data. The mode Grüneisen parameters for various modes are given in table 3. The γ_i reported in our earlier work [19] were obtained from the analysis of the data obtained from a single pressure run. Note that several modes in the low-frequency region (<50 meV) have

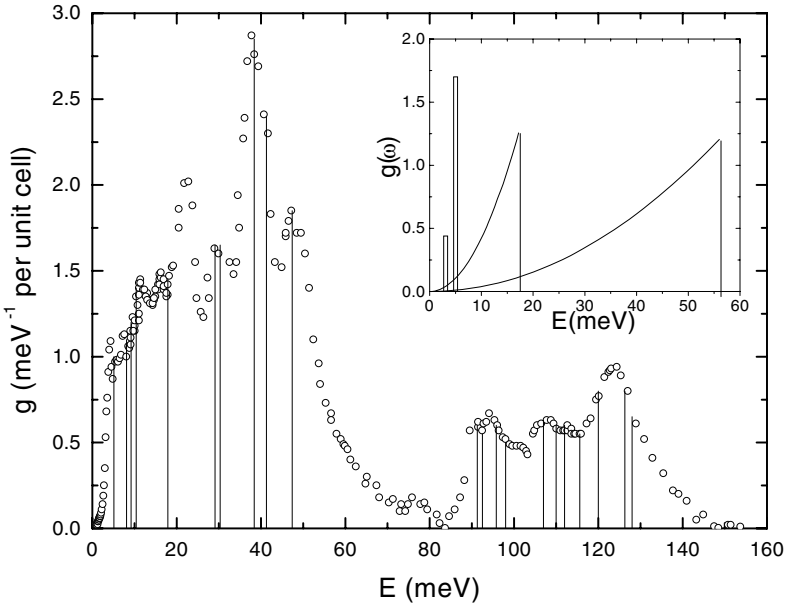

Figure 5. Comparison of reported phonon density of states $g(E)$ and observed Raman mode energies. (○) Data of Ernst *et al* [25]; vertical lines represent the positions of Raman peaks. The inset shows the density of states modelled by Ramirez and Kowach [52] for fitting the specific heat data.

negative γ_i. In view of the experimental errors the values of the Grüneisen parameter for some of the modes may be treated as either negative or zero. The modes with negative γ_i also include some of the ν_2 and ν_4 internal modes of WO_4 ion. This suggests that in addition to the lattice, rigid translational and librational modes of WO_4 ion, the distortion of the WO_4 ion arising from the soft bending modes also contributes to the mechanism of NTE. Earlier interpretations of NTE have completely ignored this aspect. The Grüneisen parameter for the lowest-frequency mode at 41 cm^{-1} (5 meV) is an order of magnitude too large as compared with typical values found in other systems. The value of γ_i for this phonon obtained from recent neutron scattering experiments [48] agrees well with that obtained in this work. Some models attribute NTE in this compound to this mode alone [25,49]. This is discussed in detail later in this paper.

In order to calculate the thermal properties such as molar specific heat C_V and α, in addition to γ_i, one also requires the number p_i of phonons/branches of frequency ω_i. We obtain this from the reported absolute phonon density of states $g(E)$ [25] (figure 5), using the procedure described earlier [19]. Note that almost all the peaks in $g(E)$ have close correspondences with the positions of the Raman lines, which are shown as vertical lines at the optical phonon energies E_i. The heights of these lines $g(E_i)$ are used for obtaining $p_i \propto g(E_i)$ such that the sums over p_i in the low- and high-energy groups have value 100 and 32 respectively. The calculated value of α at ambient temperature turns out to be -14.5×10^{-6} K^{-1}. Although an average value of -9×10^{-6} K^{-1} over the temperature range 0.3–693 K has been reported [9], an analysis of the data present in [11] yields a value of $-(11 \pm 2) \times 10^{-6}$ K^{-1} at ambient temperature. Thus the value of α obtained from the present calculation appears to be in reasonable agreement with that measured.

NTE in zirconium tungstate was originally proposed to be due to the underconstrained nature of the network structure [9] arising from the unshared vertex of WO_4 tetrahedra. A model involving transverse vibrations of Zr–O–W bonds leading to coupled librations of the

polyhedra was also proposed [11]. Early lattice dynamical calculations [49] predicted a non-Debye-like continuum of low-energy librational modes, also termed rigid-unit modes (RUM), to be responsible for NTE; however, the calculated bulk modulus turned out to be 40 times smaller than the reported value [16]. A geometrical model for the NTE in framework structures involving RUMs has also been proposed [50]. On the other hand, another lattice dynamical model [51] shows that about 40% of NTE is contributed by two transverse acoustic modes ($\gamma \sim -40$) and almost all of the NTE arises from the modes below 8 meV; however, except for energies less than 10 meV, the calculated phonon density of states [26] does not agree with the reported results [25] or with the observed [19] phonon frequencies. Measurement of specific heat up to 300 K [52] showed that at low temperature it was dominated by the contribution from a 5 meV optical phonon with associated degrees of freedom (DFs) as high as 8.5. The remaining DFs were assumed to be associated with acoustic phonons. The 5 meV optical phonon was conjectured as an evidence for the existence of RUMs. The phonon density of states was measured from inelastic neutron scattering and several low-energy phonons [25] were found. Guided by the constancy of α above 50 K, it has been argued that only phonons below 10 meV need to be considered for explaining NTE in the system. A simple model, which assumed a value of γ_i to be -14 between phonon energies 1.5 and 8.5 meV and zero otherwise, was shown [25] to fit the lattice parameter data. Subsequently, a number of fittings to the temperature dependence of lattice parameters have been performed using a variety of models [53–55] to arrive at different conclusions. Evans *et al* [53] use two Debye modes for fitting and identify a mode with characteristic Debye temperature of 95 K (8.2 meV) to have a negative Grüneisen parameter. Subsequently, the same authors [54] fitted the same data to the two-Einstein- plus two-Debye-mode model of Ramirez and Kowach [52] and found that an Einstein mode at 3.3 meV has the largest negative $\gamma_i (\sim -33)$. However, their alternative alternative analysis using the maximum-entropy method shows that a mode at 4.7 meV contributes to NTE. They consider this analysis as a direct evidence for the RUM mechanism. Subsequent analysis of the data based on two Einstein modes using a semi-empirical procedure [55] shows a mode at 4.9 or 5.8 meV to have negative γ_i. As there were no experimental data on the Grüneisen parameters of different phonon modes, these analyses had to resort to fitting to models involving a limited number of modes and treat phonon energies as well as γ_i as parameters. Only recently we have reported the mode Grüneisen parameter for phonons over a complete range of phonon energies [19] and found that in addition to the 5 meV phonon, several other phonons of energies up to 50 meV also have negative γ_i. We now analyse their contributions to the NTE.

Figure 6 shows the cumulative contribution of phonons of energies up to E to the thermal expansion $\alpha(E)$ at ambient temperature. The dips in the curve $\alpha(E)$ at 8 and 30 meV are due to positive contribution from the two phonons at these energies. Note that phonons of energies less than 8 meV contribute only 40% of the total α while the remaining 60% comes from the phonons of higher energy. This is in complete contrast with the lattice dynamical model [51] that predicted that almost all of the NTE arises from phonons of energy less than 8 meV. The present result also shows that although excellent fits to the lattice parameter data have been obtained by considering phonons only in the energy range 3–8 meV with arbitrary values [25, 53–55] of Grüneisen parameters, the phonons with energies much higher than 10 meV also contribute substantially to NTE.

It is worth examining the temperature dependence of α. Most of the available data are on lattice parameter [11, 25, 54] rather than α. The recent neutron diffraction data [54] is claimed to be of high resolution. Figure 7 shows α as a function of temperature deduced from their data. The calculated $\alpha(T)$ using the present values of γ_i is also shown for comparison. Note that apart from the differences in absolute magnitude of α at ambient temperature the

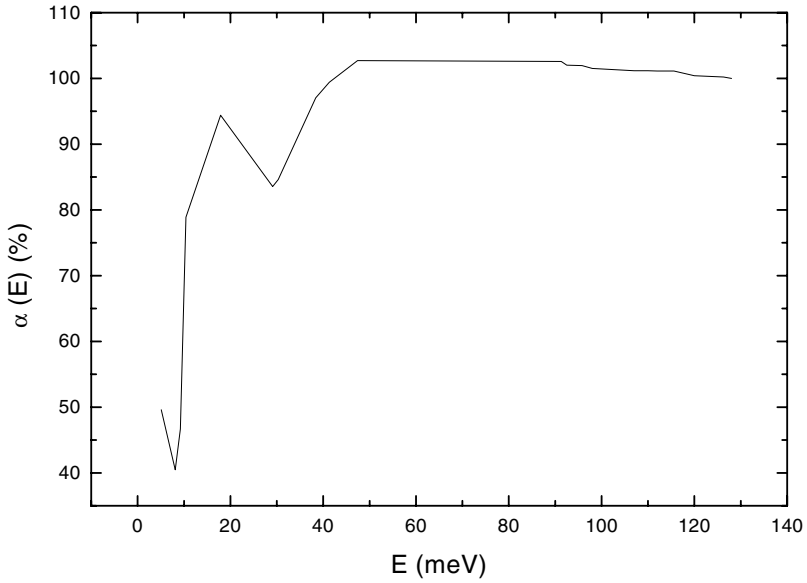

Figure 6. Cumulative contribution of the phonons of energies up to E to the thermal expansion $\alpha(E)$ at ambient temperature.

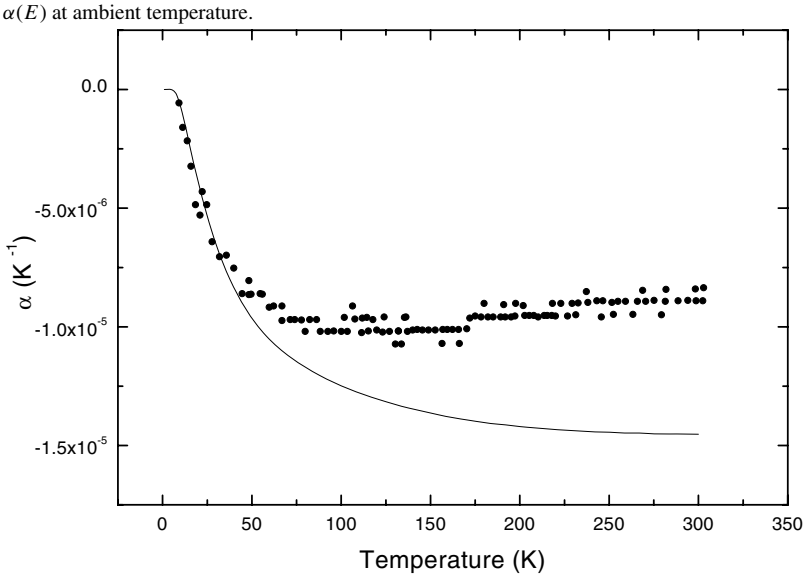

Figure 7. Temperature dependence of α calculated from the optical phonon mode Grüneisen parameters and the p_i obtained from the density of states shown in figure 5. The symbols represent the values of α extracted from the lattice parameter data of David *et al* [54].

data and the calculated curve show a similar decrease at low temperatures. The data exhibit a departure from constancy below 75 K whereas the calculated curve deviates significantly from the ambient-temperature value below 150 K. The slower decrease of the calculated α arises from the contribution of all the phonons. It has recently been argued that the temperature dependence of α could arise only from modes below 10 meV [56]. On the other hand, the contribution of the phonons of energy higher than 10 meV has also been unambiguously established [57].

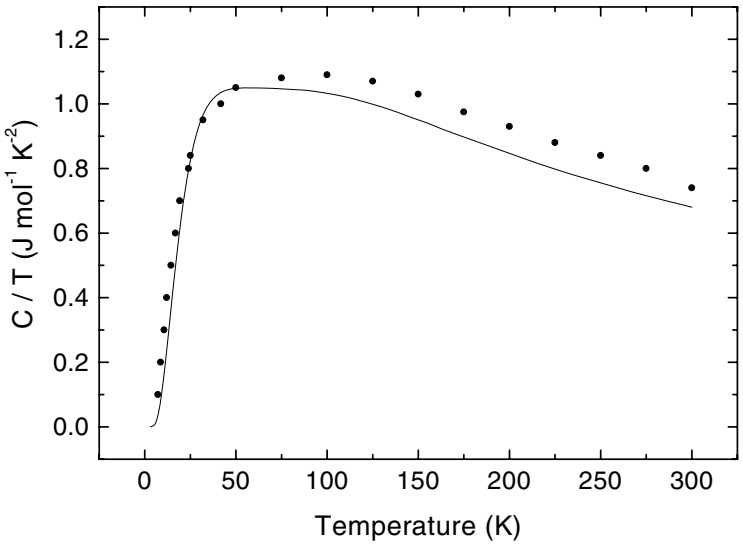

Figure 8. Temperature dependence of the specific heat calculated from the optical phonon frequencies and the p_i obtained from the density of states shown in figure 5. Symbols represent the data of Ramirez and Kowach [52].

As mentioned earlier, guided by examples of a few network systems, which exhibit both NTE and PIA, a possibility of a common origin [18,37] between the two phenomena has been speculated. NTE necessarily implies that some of the modes have negative γ_i and this in turn suggests instability of the present structure against a structural change and not necessarily amorphization. On the other hand, PIA arises either due to kinetic hindrance of equilibrium phase transition or due to kinetic hindrance of equilibrium decomposition. PIA is observed more frequently in network systems than other systems because of the sluggishness of a structural transition or decomposition. Thus PIA is a consequence of slow kinetics, while NTE is correlated to structural instability. On the other hand, a structural instability does not necessarily imply NTE. In view of this the correlation between NTE and PIA, if any, may be only marginal.

3.5. Specific heat

As discussed earlier, zirconium tungstate has as many as 129 DFs distributed among optical phonons and the remaining three DFs account for the acoustic phonons. Partial density of states obtained from lattice dynamics [26] calculations shows that the acoustic phonons arising from the translational motion of Zr atoms are of moderate energy. The knowledge of optical phonon frequencies allows one to take into account their contribution to the specific heat. In order to confirm whether the measured phonon frequencies and the corresponding DFs, used in the calculation of α, also reproduce the value of the specific heat, we calculate the molar specific heat at ambient temperature to be 200 J mol^{-1} K^{-1}. This is in good agreement with the measured value [52] of 220 J mol^{-1} K^{-1}. One can also examine the temperature dependence of C_V and compare with reported results. For this a Debye contribution arising from the acoustic phonons with three DFs and Debye temperature $\theta_D = 200$ K (17.2 meV) is also considered. Figure 8 shows C_V/T as a function of temperature along with the data [52] of Ramirez and Kowach. Note the good agreement between the calculated and the reported data

over the complete range of temperature. However, it must be pointed out that an excellent fit to C_V had also been obtained by Ramirez and Kowach using a model incorporating two Debye plus two Einstein modes with arbitrary values [52] of mode energies and oscillator strengths. They use a Debye mode of cut-off energy 56 meV with DF (DF $= 4\times$ oscillator strength) as high as 90 assigned to it. In fit 2 another Debye mode of 17.2 meV with 28.8 DF is added to the first mode, whereas the low-energy Einstein modes were assigned a total DF less than nine. The inset to figure 5 shows the density of states according to their model. Note that this manner of distributing the DF is thus opposite to the manner in which the optical and acoustic phonons actually exist in the system. This can be further confirmed from the complete disagreement between the density of states represented by their model and the reported $g(E)$. Thus the present arguments show that the parameters that yielded the good fit were unphysical; and the data can be satisfactorily explained if the density of states arising from the optical phonons is properly taken into account. One can improve the agreement by incorporating minor changes in the values of DF such that total DF is conserved.

4. Summary and conclusions

Raman spectroscopic measurements were carried out on zirconium tungstate at high pressure. Mode Grüneisen parameters of several phonons were found to be negative. In addition to the low-frequency RUM, the bending distortions of the tungstate tetrahedra also appear to contribute to the mechanism of NTE in this system. The temperature dependence of the coefficient of thermal expansion and the molar specific heat calculated according to the present model agrees well with the reported data. The analysis of the cumulative $\alpha(E)$ strongly suggests that the optical phonons of energies much higher than 8 meV also contribute substantially to NTE. The present measurements confirm the lowering of symmetry across the α–γ transition and coexistence of phases between 0.2 and 0.5 GPa. The pressure-induced amorphization occurring at 2.2 ± 0.3 GPa is shown to arise from the kinetic hindrance of equilibrium decomposition in a mixture of oxides.

Acknowledgments

TRR and AKA wish to thank Dr T S Radhakrishnan for interest in the work, Dr Baldev Raj for support and Mr S B Bhoje for encouragement. TAM also thanks Dr S Venugopal, Dr S K Ray and Dr S L Mannan for support.

References

[1] Blackman M 1957 *Proc. Phys. Soc.* B **70** 827
[2] Rottger K, Endriss A, Ihringer J, Doyle S and Kuhs W F 1994 *Acta Crystallogr.* B **50** 644
[3] White G K 1978 *J. Phys. C: Solid State Phys.* **11** 2171
[4] Herona K, Maeta H, Ohashi K and Koike T 1986 *J. Phys. C: Solid State Phys.* **19** 5149
[5] Taylor D 1984 *Br. Ceram. Trans. J.* **83** 129
[6] Taylor D 1986 *Br. Ceram. Trans. J.* **85** 147
[7] Shirone G and Hoshina S 1951 *J. Phys. Soc. Japan* **6** 265
[8] Martinek C and Hummel F A 1968 *J. Am. Ceram. Soc.* **51** 227
[9] Mary T A, Evans J S O, Vogt T and Sleight A W 1996 *Science* **272** 90
[10] Foster P M and Sleight A W 1999 *Int. J. Inorg. Mater.* **1** 123
[11] Evans J S O, Mary T A, Vogt T, Subramanian M A and Sleight A W 1996 *Chem. Mater.* **8** 2809
[12] Lind C, Wilkinson A P, Hu Z, Short S and Jorgensen J D 1998 *Chem. Mater.* **10** 2335
[13] Evans J S O and Mary T A 2000 *Int. J. Inorg. Mater.* **2** 143
[14] Yamamura Y, Nakajima N and Tsuji T 2000 *Solid State Commun.* **114** 453

[15] Evans J S O, Hu Z, Jorgensen J D, Argyriou D N, Short S and Sleight A W 1997 *Science* **275** 61
[16] Jorgensen J D, Hu Z, Teslic S, Argyriou D N, Short S, Evans J S O and Sleight A W 1999 *Phys. Rev.* B **59** 215
[17] Pryde A K A, Dove M T and Heine V 1998 *J. Phys.: Condens. Matter* **10** 8417
[18] Perottoni C A and da Jornada J A H 1998 *Science* **280** 886
[19] Ravindran T R, Arora A K and Mary T A 2000 *Phys. Rev. Lett.* **84** 3879
Ravindran T R, Arora A K and Mary T A 2000 *Phys. Rev. Lett.* **85** 225
[20] Ravindran T R and Arora A K 1999 *High Press. Res.* **16** 233
[21] Hanuza J and Macalik L 1987 *Spectrochim. Acta* A **43** 361
[22] Turrel G 1972 *Infrared and Raman Spectra of Crystals* (New York: Academic)
[23] Herzberg G 1962 *Molecular Spectra and Molecular Structure* vol 2 (New York: van Nostrand-Reinhold)
[24] Scott J F 1968 *J. Chem. Phys.* **48** 874
[25] Ernst G, Broholm C, Kowach G R and Ramirez A P 1998 *Nature* **396** 147
[26] Mittal R and Chaplot S L 2000 *Solid State Commun.* **115** 319
[27] Amores J M G, Amador U, Moran E and Franco M A A 2000 *Int. J. Inorg. Mater.* **2** 123
[28] Evans J S O, Jorgensen J D, Short S, David W I F, Ibberson R M and Sleight A W 1999 *Phys. Rev.* B **60** 14 643
[29] Weinstein B A and Zallen R 1984 *Light Scattering in Solids* vol 4, ed M Cardona and G Güntherodt (Berlin: Springer) p 463
[30] Batlogg B, Jayaraman A, van Cleve J E and Maines R G 1983 *Phys. Rev.* B **27** 3920
[31] Arora A K 1990 *J. Phys. Chem. Solids* **51** 373
[32] Sakuntala T, Arora A K, Shekar N V C and Sahu P Ch 1998 *Europhys. Lett.* **44** 728
[33] Klug D D, Mishima O and Whalley E 1986 *Physica* B **139–40** 475
[34] Arora A K and Sakuntala T 1992 *J. Phys.: Condens. Matter* **4** 8697
[35] Hemley R J, Jephcoat A P, Mao H K, Ming L C and Manghnani M H 1988 *Nature* **334** 52
[36] Mishima O, Calvert L D and Whalley E 1984 *Nature* **310** 393
[37] Speedy R J 1996 *J. Phys.: Condens. Matter* **8** 10 907
[38] Bassett W A and Ming L C 1972 *Phys. Earth Planet. Inter.* **6** 154
[39] Hegenbart W, Rau F and Range K J 1981 *Mater. Res. Bull.* **16** 413
[40] Kato T, Kubo T, Morishima H, Ohtani E, Suzuki A, Yamazaki D, Mibe K, Kikegawa T and Shimomura O 1998 *Rev. High Press. Sci. Technol.* **7** 119
[41] Richard G and Richet P 1990 *Geophys. Res. Lett.* **17** 2093
[42] Jayaraman A, Wang S Y, Ming L C and Cheong S W 1995 *Phys. Rev. Lett.* **75** 2356
[43] Guyot F and Reynard B 1992 *Chem. Geol.* **96** 411
[44] Arora A K 2000 *Solid State Commun.* **115** 665
[45] Arora A K and Sakuntala T 2000 *High Press. Res.* **17** 1
[46] Kuzmin A, Purans J, Cassanelli E, Vinegoni C and Mariotto G 1998 *J. Appl. Phys.* **84** 5515
[47] Carlson S and Anderson A M K 2000 *Phys. Rev.* B **61** 11 209
[48] Mittal R, Chaplot S L, Schober H and Mary T A 2001 *Phys. Rev. Lett.* **86** 4692
[49] Pryde A K A, Hammonds K D, Dove M T, Heine V, Gale J D and Warren M C 1996 *J. Phys.: Condens. Matter* **8** 10 973
[50] Heine V, Velche P R L and Dove M T 1999 *J. Am. Ceram. Soc.* **82** 1973
[51] Mittal R and Chaplot S L 1999 *Phys. Rev.* B **60** 7234
[52] Ramirez A P and Kowach G R 1998 *Phys. Rev. Lett.* **80** 4903
[53] Evans J S O, David W I F and Sleight A W 1999 *Acta Crystallogr.* B **55** 333
[54] David W I F, Evans J S O and Sleight A W 1999 *Europhys. Lett.* **46** 661
[55] Wang K and Reeber R R 2000 *Appl. Phys. Lett.* **76** 2203
[56] Chaplot S L and Mittal R 2001 *Phys. Rev. Lett.* **86** 4976
[57] Ravindran T R and Arora A K 2001 *Phys. Rev. Lett.* **86** 4977